Polymer Vol. 39 No. 26, pp. 6861–6874, 1998

0032-3861/98/$ - see front matter

PII: S0032-3861(98)00135-9

Segmented block copolymers of natural rubber and 1, 3-butanediol–toluene diisocyanate oligomers

C. J. Paul[a], M. R. Gopinathan Nair[a,*], N. R. Neelakantan[b], Peter Koshy[c], Bhaskar B. Idage[d] and A. A. Bhelhekar[d]

[a]*School of Chemical Sciences, Mahatma Gandhi University, Priyadarshini Hills, Kottayam, 686 560 Kerala, India*
[b]*Chemical Engineering Division, Indian Institute of Technology, Madras 600 036, India*
[c]*Instrumentation and Electron Microscopy Division, Regional Research Laboratory, Trivandrum 695 019, India*
[d]*National Chemical Laboratory, Pune 411008, India*
(Revised 12 December 1997)

A series of segmented block copolymers of NR and 1,3-butanediol–toluene diisocyanate oligomers have been synthesized with varying hard segment content. The synthesis has been carried out by one-shot and two-shot processes in solution. The products were characterized by spectral analysis, thermal and mechanical analysis, SEM and optical microscopy. They are found to be amorphous materials having no potential for hydrogen bonding between the 'hard' and 'soft' segments. Their two-phase morphology has been deduced from SEM and optical micrographs and established by DMA and thermal studies. DSC analysis shows a soft segment glass transition temperature at -62 ± 2°C and hard segment glass transitions between 70° and 100°C, depending on the polyurethane content. The T_g values determined by the dynamic mechanical analysis are significantly higher than these values.

The thermogravimetric analysis indicates a two-stage thermal decomposition of the materials by random nucleation mechanism and corresponds to the two phases present in the block copolymer. Depending on the proportion of the continuous and dispersed phases, the block coolymers behave like quasi-elastomers at lower hard segment concentrations and brittle plastics at higher hard segment contents. This variation in mechanical behaviour is consistent with the sample morphology. Materials synthesized by the two-shot process are found to possess better mechanical properties than the one-shot products, presumably due to a more systematic ordering of the different segments in the former.

(Keywords: liquid natural rubber; polyurethanes; segmented block copolymer)

INTRODUCTION

The great commercial importance of thermoplastic elastomers has stimulated a great number of investigations into the production and the structure–property analysis of segmented block copolymers. Their unusual properties are attributed to the incompatibility and the subsequent formation of a microphase-separated domain structure consisting of hard and soft phases.[1–6] However, conventional polyurethane block copolymers have extensive physical and thermodynamic interactions between the two phases. This restricts the studies on the structure–property relations existing in these materials. Hence the use of polydienes[4,7–15] and polyolefins[16,17] as soft segment aroused special interest and a good number of studies have been reported in recent times. These block copolymers are model systems in which the hydrogen bonding and other types of interactions are limited to the hard segment. The nonpolar soft segments form a separate phase and phase mixing with the hard segment is totally absent in these block copolymers. The nonpolar nature of the soft segments causes low moisture permeability and hence they have found use in the development of adhesives and electrical potting compounds.

A series of block copolymers with NR soft segments have been examined in some studies reported earlier.[6,18,19] The NR soft segment has been derived from hydroxyl terminated liquid natural rubber made by the depolymerization of NR. This has a number average molecular weight of 3500 and average functionality 1.90. This has been chain extended with polyurethane from toluene diisocyanate (80:20 mixture of 2, 4- and 2, 6-isomers) and 1, 4-butanediol[6] and also with polyethylene oxide.[19] The morphology and thermal transitions have been assessed and it was found that they are typical of a completely phase-segregated system. Block copolymers of NR and polyurethane formed from TDI and ethylene glycol have been synthesized and reported recently from our laboratory.[20] These samples were made by both one-shot and two-shot processes in solution. The properties varied from soft to rigid elastomers and rubber toughened plastics as the hard segment content increased from 30% to 70%. However, the mechanical properties were found to be inferior to earlier systems consisting of butanediol–toluene diisocyanate hard segments. The sample morphology was consistent with a two-phase system. The hard phase in the

* To whom correspondence should be addressed

one-shot materials is spherical in shape with a wide particle size distribution, whereas the two-shot products are found to have elliptical shape and a more or less uniform size distribution.

The present work is an attempt to synthesize and characterize a series of block copolymers of NR with a different hard segment consisting of 1, 3-butanediol and toluene diisocyanate. It is interesting to note the change in properties of the block copolymers with the variation in the structure of polyurethane hard segment. The samples were synthesized by one-shot and two-shot processes in solution and the percentage of hard segment varies from 30% to 70%.

EXPERIMENTAL

Materials

Hydroxyl-terminated liquid natural rubber (HTNR) with number average molecular weight 3500 was prepared in the laboratory by the photochemical degradation[21] of natural rubber of ISNR5 grade supplied by the Rubber Research Institute of India, Kottayam. Toluene diisocyanate (TDI) (80:20 mixture of 2, 4- and 2, 6-isomers) was obtained from Fluka, Switzerland and was used as received. 1, 3-Butanediol (1, 3-BDO) and dibutyl tin dilaurate (DBTDL) were also obtained from Fluka. Tetrahydrofuran (THF), BDH, was dried by using sodium wire and distilled before use.

Synthesis of block copolymers

The polyurethane block copolymers were synthesized by both one-shot and two-shot solution polymerization techniques.

One-shot process

The stoichiometric amounts of HTNR and 1, 3-butanediol were dissolved in THF to get 25% solution. DBTDL (about 0.03% by weight of HTNR) was added as catalyst and the solution was taken in a flat bottomed flask equipped with a magnetic stirrer, reflux condenser and a dropping funnel. The final desired quantity of TDI was dropped into it over a period of 45 min at reflux temperature with constant stirring. A 2% excess TDI was added in order to compensate for any loss during the process. The reaction is continued for 3 h. The excess THF was distilled off and the viscous polymer solution was cast in trays treated with silicon release agent and kept for curing at 70°C for 24 h followed by two weeks aging at room temperature in a dry atmosphere.

Two-shot process

The stoichiometric amounts of HTNR was dissolved in THF to get a 20% solution. DBTDL (about 0.03% by weight of HTNR) was added and the solution was taken in a flat bottomed flask equipped with a magnetic stirrer, reflux condenser and a dropping funnel. It was refluxed at 80°C. TDI in THF was added dropwise with constant stirring and the reaction was continued for 2 h to ensure endcapping of HTNR. The required quantity of 1, 3-BDO in THF (20%, w/v) was then added over a period of 45 min. The reaction was continued for 3 h and the excess THF was distilled off. The viscous polymer solution was then cast, cured and aged as above.

Polymer designation

The samples are designated as follows. As an example NR/1, 3-BDO (70/30) indicates 70% by weight of HTNR and 30% by weight of polyurethane based on 1, 3-BDO and 2, 4-TDI. The overall compositions of the block copolymers are summarized in *Table 1*.

Table 1 The overall composition of the block copolymers

Sample	Molar composition, HTNR/TW/1, 3-BDO	Polyurethane content (%)
NR/1, 3-BDO(70/30)	1/5.97/4.86	33.00
NR/1, 3-BDO(60/40)	1/8.74/7.57	42.35
NR/1, 3-BDO(50/50)	1/12.60/11.35	51.17
NR/1, 3-BDO(40/60)	1/18.39/17.03	61.23
NR/1, 3-BDO(70/70)	1/27.04/26.49	70.28

Measurements

IR spectra of the samples were recorded on a Shimadzu IR-470 infrared spectrometer. The ^{1}H n.m.r. spectra were recorded on a Bruker AC 200 MHz FTNMR and ^{13}C n.m.r. on a Bruker AC 50 MHz spectrometer. A Perkin Elmer Delta Series DSC 7 calorimeter and a Mettler Iric (TA 3000) microcalorimeter were used to characterize the thermal properties of the samples. The samples were scanned at a heating rate of 10°C min^{-1} and at a sensitivity of 5 mcal s^{-1}. The thermogravimetric analysis was performed by a Perkin-Elmer TGA 7 and a Shimadzu-DT-40 thermal analysers at a scanning rate of 10°C min^{-1}. The dynamic mechanical measurements (DMA) were carried out by a processor controlled Rheovibron, model RHEO-426B DDV TIC (Japan) at a fixed frequency of 35 Hz. Samples are heated at a nominal rate of 1.5°C min^{-1} under dry nitrogen atmosphere. The fracture surfaces of samples from tensile tests were sputter coated with gold and examined on a JEOL JSM-35C scanning electron microscope. Optical micrographs of thin films of the samples were taken on a 'Leitz' Orthoplan microscope at a magnification of 100×. Dumbbell shaped test specimen were machined from cast sheets and tested on a Zwick 1474 universal testing machine (UTM) as per ASTM D412-80 test method at 25°C at a constant crosshead speed of 500 mm min^{-1}. Tear strength of the samples was tested on Zwick 1474 UTM as per ASTM D624-81 using a nicked 90° angle specimen.

RESULTS AND DISCUSSION

The block copolymers prepared by the two-shot and one-shot processes were analysed by IR spectroscopy and the results are presented in *Figures 1 and 2*, respectively. *Figure 1* includes the IR spectra of HTNR (*Figure 1a*), –NCO endcapped liquid NR (*Figure 1b*), polyurethane hard segment prepared by the reaction of TDI and 1, 3-BDO (*Figure 1c*), and the block copolymer by two-shot process (*Figure 1d*). The endcapping of HTNR and the subsequent chain extension in the two-shot process are clearly followed in these spectra. *Figure 2* indicates the progress of the reaction during the one-shot process. Absence of the band at 2260 cm^{-1} in *Figure 2d* shows the product contains no residual diisocyanate. These results are consistent with the course of reaction given in *Schemes 1* and *2* for one-shot and two-shot processes, respectively. It was found that the IR spectra, viz. *Figure 1d* and 2*d*, of the block copolymers under discussion are identical irrespective of the composition and history of synthesis, indicating similar chemical composition of the final products in the one-shot and two-shot processes.

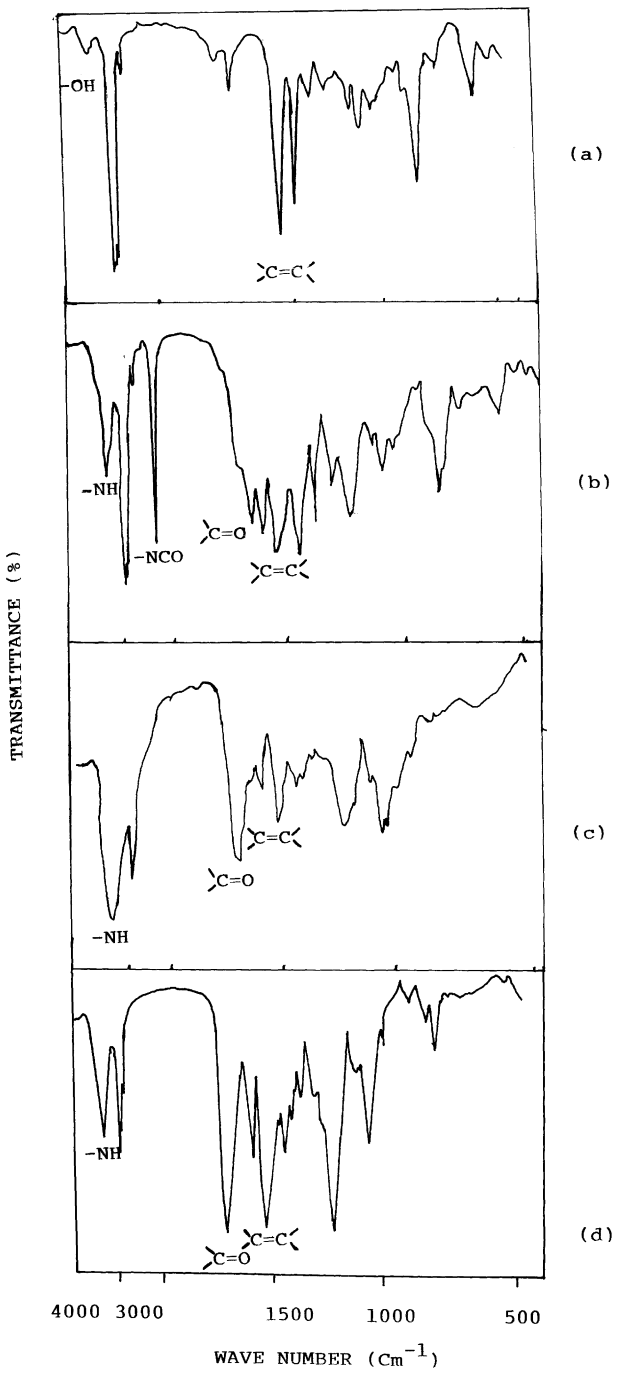

Figure 1 IR spectra of: (a) HTNR; (b) –NCO endcapped NR; (c) 1, 3-BDO based polyurethane hard segment; (d) block copolymer by two-shot process.

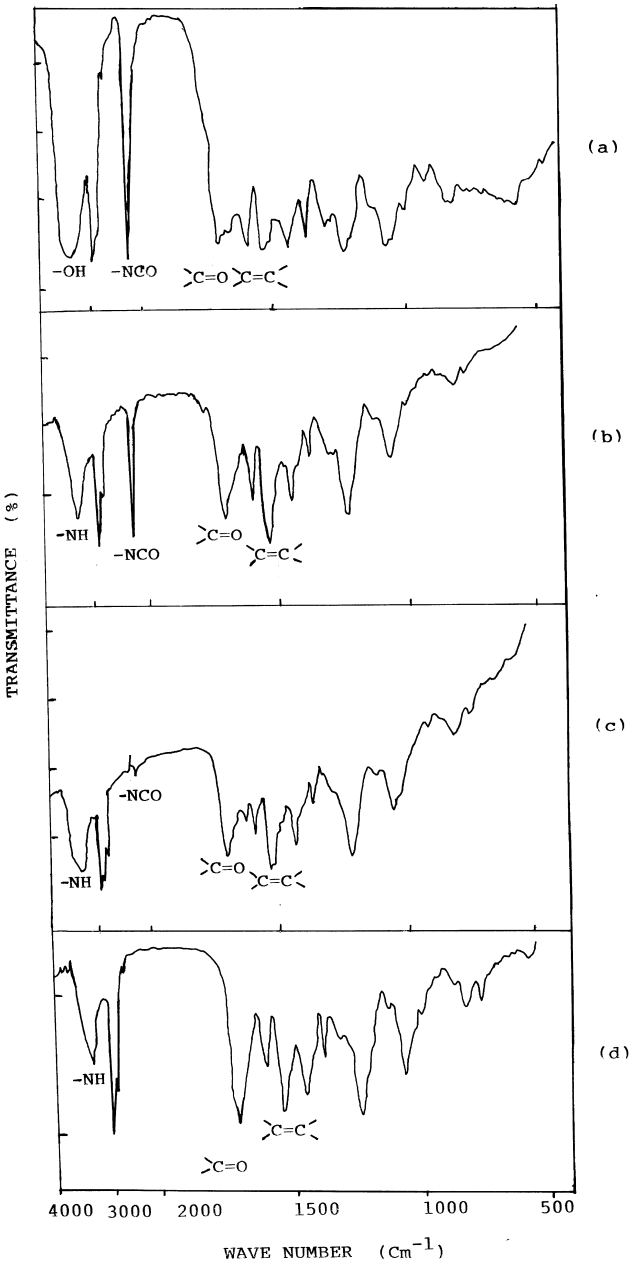

Figure 2 IR spectra at different intervals of the reaction (for NR/1, 3-BDO (50/50) by one-shot process): (a) at the beginning of addition of TDI; (b) after 1 h; (c) after 3 h; (d) after 4 h.

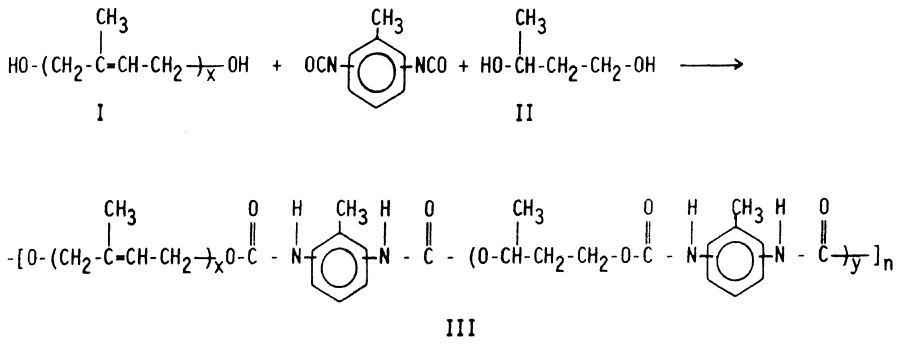

Scheme 1 The course of the reaction and the structure of the product (one-shot process).

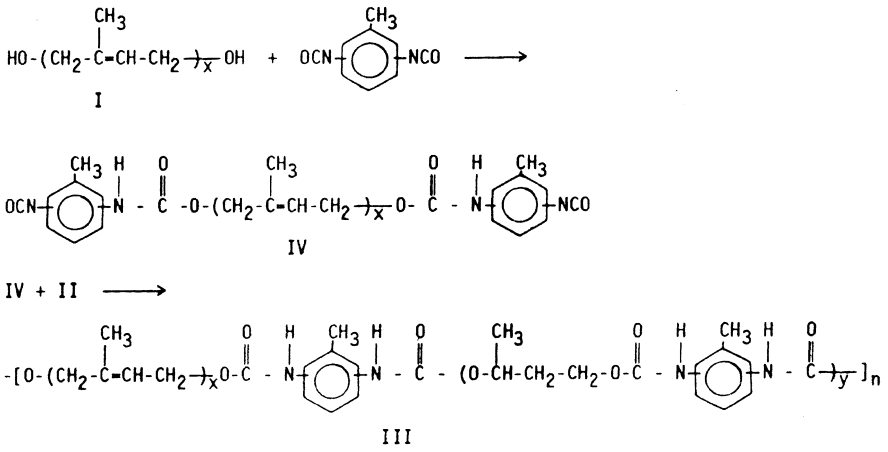

Scheme 2 The course of the reaction and the structure of the product (two-shot process).

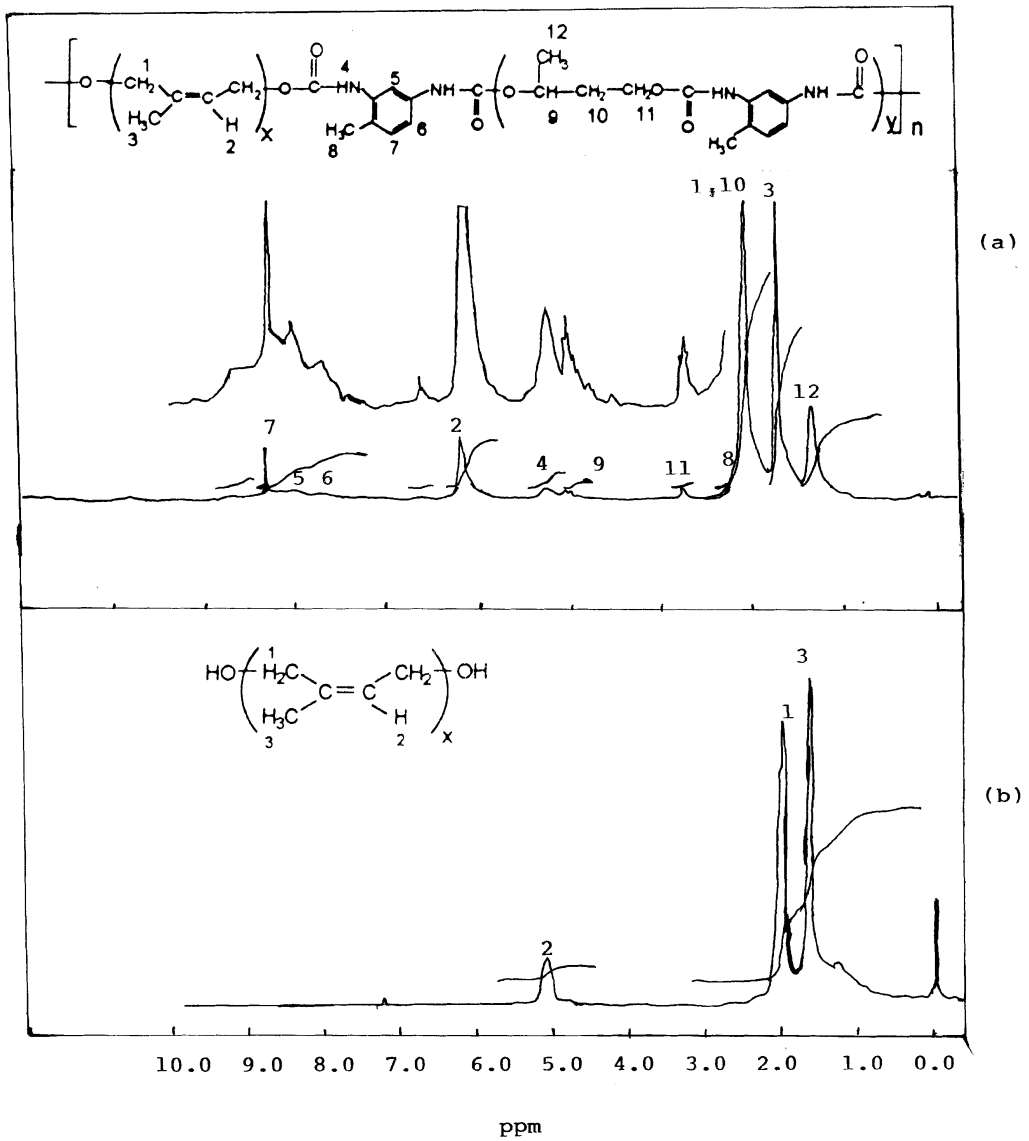

Figure 3 ^{1}H-NMR spectra of: (a) NR/1, 3-BDO (50/50) by one-shot process; (b) HTNR.

The ^{1}H n.m.r. and ^{13}C spectra of the products support the IR spectra in characterizing the features of the soft and hard segments. The spectra of one-shot and two-shot samples were found to be identical. *Figure 3a* is the ^{1}H n.m.r. spectrum of NR/1, 3-BDO (50/50) and *Figure 3b* is that of HTNR. The ^{13}C spectrum of NR/1, 3-BDO (50/50) is given in *Figure 4*, which includes the features of the hard and soft segments. Apart from the major peaks the spectra also

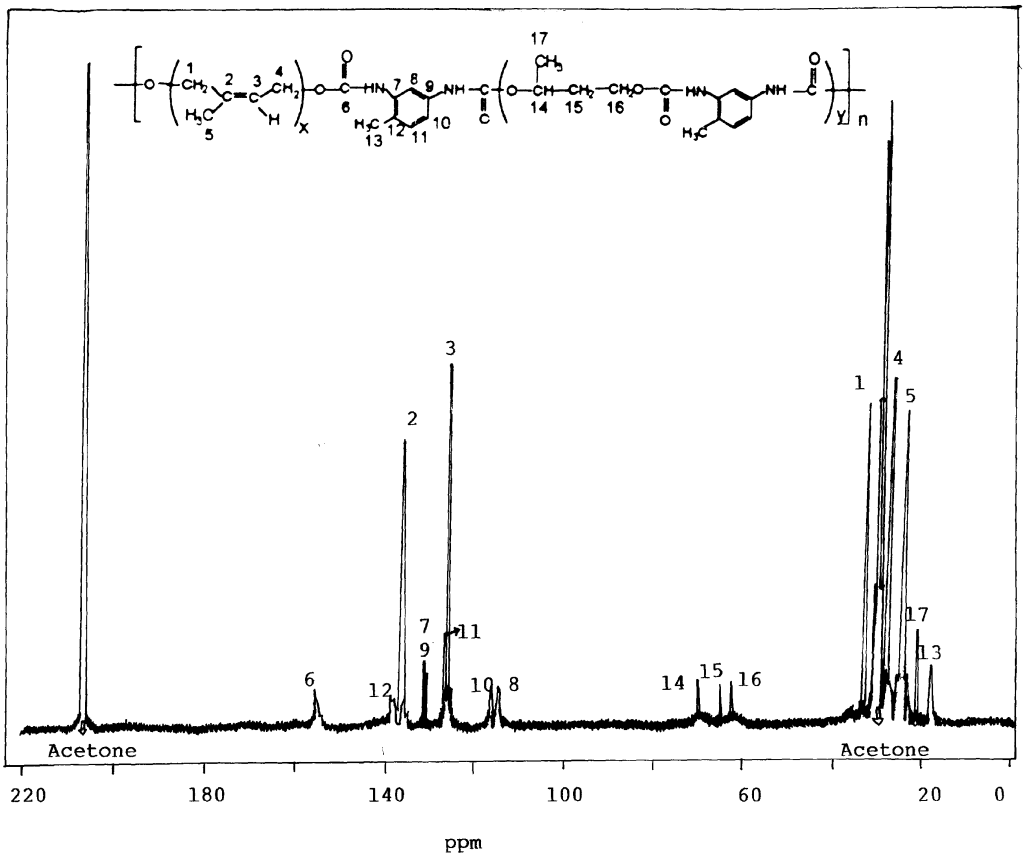

Figure 4 ^{13}C NMR spectrum of NR/1, 3-BDO (50/50) by two-shot process.

contain some minor peaks which may be due to the presence of some probable side products and certain allophanate linkages. It is observed that the peaks characteristic of the hard segments are relatively weak compared with those of the soft segment. The low solubility and hence the low mobility of the hard segments (due to H-bonding) in the solvent may account for this observation.

Differential scanning calorimetry (DSC)

Differential scanning calorimetric analysis of selected products has been carried out and the thermograms are given in *Figures 5 and 6*, respectively, for one-shot and two-shot samples. The observed glass transition temperatures are tabulated in *Table 2*.

The soft segment glass transition is well defined and appears at $-62.4 \pm 2°C$ (*Figure 5b*). This value is almost a constant, since the HTNR segments are common to all the presently studied systems, and is found to be independent of hard segment content, in contrast to the conventional polyurethanes which exhibit appreciable interphase interactions. This soft segment T_g is very close to that observed for the homopolymer HTNR (−68°C). The variation is 3–4° above that of free HTNR. Camberlin and Pascault[14] have calculated that a rise of 4° in T_g of the corresponding homopolymer indicates complete or almost complete phase separation and confirms the two-phase nature of the products.

Single hard segment T_g values are observed for all samples irrespective of the method of synthesis (i.e. one-shot or two-shot method). It varies with variation in the hard segment content. However, there is no linear relationship between T_g and inverse number average molecular weights of the hard segments in the TDI/1, 3-BDO polyurethane systems.[22] Observation of a single hard segment transition for all the samples is consistent with the fact that the hard segments have a very narrow molecular weight distribution. It is also observed that there is no appreciable difference in T_g values between the one-shot and two-shot products.

Table 2 Glass transition temperature of the hard segments observed in the DSC thermogram

Sample	T_g of the hard segment	
	One-shot (°C)	Two-shot (°C)
NR/1, 3-BDO (60/40)	73.53	72.20
NR/1, 3-BDO (50/50)	76.43	79.00
NR/1, 3-BDO (40/60)	83.33	87.02
NR/1, 3-BDO (30/70)	86.40	–

Thermogravimetry

The thermal stability of the block copolymers were studied using thermogravimetric analysis (TGA). *Figure 7* shows typical thermograms of the one-shot products and *Figure 8* those of the two-shot products. The onset of weight loss, the DTG peak temperatures and the percentage of mass loss in each stage are summarized in *Tables 3* and *4* for one-shot and two-shot products, respectively.

All the copolymers decomposed in two stages corresponding to the two phases present. In most cases the onset of weight loss occurred between 205 and 215°C. The first step decomposition was complete in the temperature range of 340–354°C. The percentage of mass loss in this step decreases as the hard segment content decreases indicating that the first stage decomposition is due to the hard segment. The second decomposition was rather rapid and was

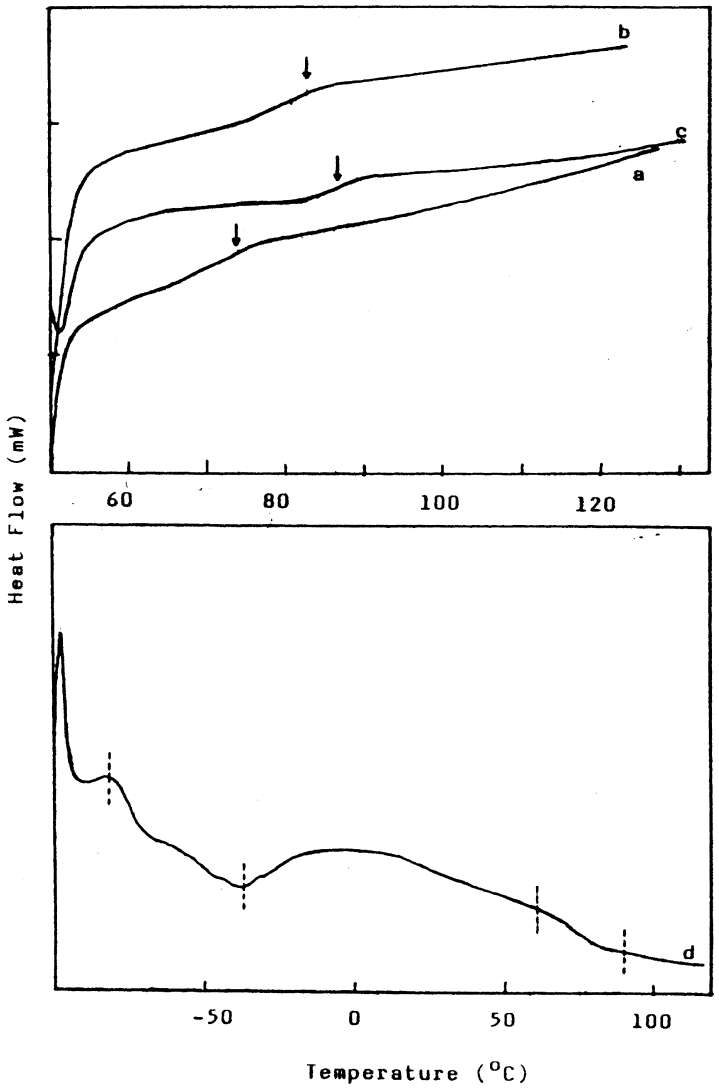

Figure 5 DSC thermograms of typical one-shot products: (a) NR/1, 3-BDO (60/40) (Perkin-Elmer analyser); (b) NR/1, 3-BDO (40/60) (Perkin-Elmer analyser); (c) NR/1, 3-BDO (30/70) (Perkin-Elmer analyser); (d) NR/1, 3-BDO (50/50) (Mettler analyser).

Table 3 Phenomenological data of thermal decomposition of the one-shot products

Sample	Onset of weight loss (°C)	Percentage of mass loss		Peak temperature from DTG curves (°C)	
		Stage 1	Stage 2	Stage 1	Stage 2
NR/1, 3-BDO (70/30)	250.0	35.90	63.70	275.0	401.0
NR/1, 3-BDO (60/40)	264.3	39.61	60.46	304.6	396.6
NR/1, 3-BDO (50/50)	268.5	49.04	50.62	309.3	394.2
NR/1, 3-BDO (40/60)	277.3	54.79	45.25	316.4	394.6
NR/1, 3-BDO (30/70)	235.0	64.00	36.00	284.0	398.0

complete around 440°C. This is attributed to the decomposition of the soft segment. A plateau of temperature separated the two stages of decomposition which indicates the decomposition of the two phases at different temperatures.

Thermal decomposition kinetics of the block copolymers from the T_g curves

The kinetic parameters for the decomposition of the blockcopolymers are calculated from the T_g curves by the integral method reported by Madhusudanan *et al.*[23] using the least square method. The integral equation used has the form:

$$\ln g(\alpha)/T^2 = \ln[AR/\phi E(1 - 2RT/E) - E/RT] \qquad (1)$$

where A is the pre-exponential factor (Arrhenius parameter) which is calculated from the intercept using the relation, intercept $= \ln AR/\phi E$, where R = the universal gas constant, E = the energy of activation, T = the absolute temperature. The entropy of activation, ΔS, is calculated using the relation:

$$A = KT_s/h \cdot e^{\Delta S/R}$$

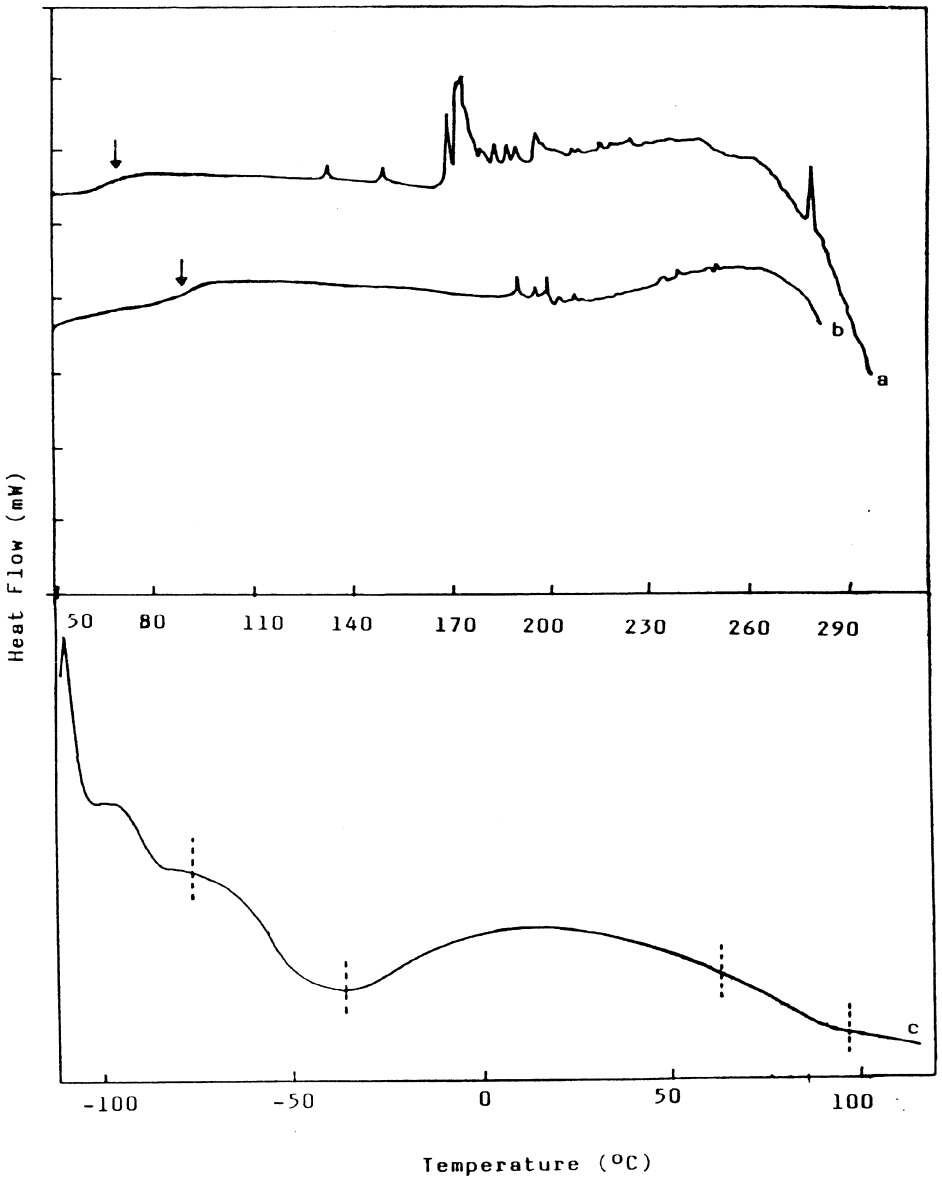

Figure 6 DSC thermograms of typical two-shot products: (a) NR/1, 3-BDO (60/40) (Perkin-Elmer analyser); (b) NR/1, 3-BDO (40/60) (Perkin-Elmer analyser); (c) NR/1, 3-BDO (50/50) (Mettler analyser).

Table 4 Phenomenological data of thermal decomposition of the two-shot products

Sample	Onset of weight loss (°C)	Percentage of mass loss		Peak temperature from DTG curves (°C)	
		Stage 1	Stage 2	Stage 1	Stage 2
NR/1, 3-BDO (70/30)	203.0	36.00	63.70	287.0	376.0
NR/1, 3-BDO (60/40)	208.0	39.90	57.30	275.0	415.0
NR/1, 3-BDO (50/50)	198.0	50.10	49.90	277.0	412.0
NR/1, 3-BDO (40/60)	201.0	58.00	42.00	286.0	372.0
NR/1, 3-BDO (30/70)	196.0	67.00	33.00	282.0	395.0

where K = the Boltzmann constant, T_s = the peak temperature in the DTG curve, and h = Planck's constant.

A plot of the left-hand side of equation (1) versus the reciprocal of the temperature gives a straight line with slope $-E/R$.

Several mechanistic equations have been derived from the integral equation by different authors to determine the decomposition kinetics. Satava[24] has chosen nine equations based on nine different mechanisms (i.e. nine different forms of $g(\alpha)$).

All the T_g data have been analysed using the nine mechanistic equations. It is observed that, irrespective of the composition and method of synthesis of the block copolymers, the highest correlation coefficient is obtained from the equation $-\ln(1-\alpha) = kt$ (Mampel). Thus the Mampel equation best represents the experimental data and gives the proper mechanism of the reaction. Hence it may be

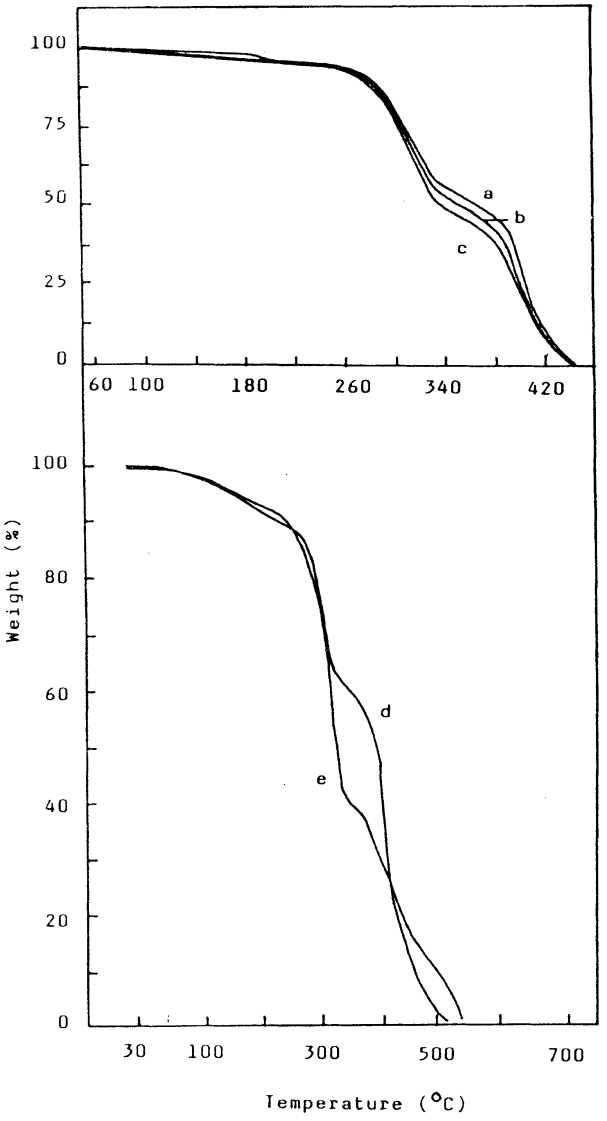

Figure 7 Thermograms of the one-shot products from TGA analysis: (a) NR/1, 3-BDO (60/40) (Perkin-Elmer analyser); (b) NR/1, 3-BDO (50/50) (Perkin-Elmer analyser); (c) NR/1, 3-BDO (40/60) (Perkin-Elmer analyser); (d) NR/1, 3-BDO (70/30) (Shimadzu analyser); (e) NR/1,3-BDO(30/70) (Shimadzu analyser).

concluded that the thermal decomposition of the segmented block copolymers follows a random nucleation mechanism. The kinetic parameters calculated from the T_g curves of one-shot and two-shot products are summarized in *Tables 5* and *6*, respectively.

Dynamic mechanical measurements

The temperature dependences of the storage and loss modulii (E' and E'') for the one-shot samples and the two-shot samples are represented in *Figures 9 and 10*, respectively. The corresponding plots of tanδ versus temperature are given in *Figures 11 and 12*. The two types of samples show a major relaxation at about −37°C characterized by a decrease in storage modulus of at least two orders of magnitude. This is attributed to the glass transition of the NR segments. This T_g value is unaffected by the urethane content, indicating that the soft segment phase is well separated and the material is a two-phase system. The E'' curves show a second peak or shoulder at a higher temperature which increases in magnitude with increasing hard segment content. This effect is marked in the case of the two-shot samples. It is only reasonable to believe that this second relaxation is due to the hard segments.

Table 7 summarizes the relaxation values obtained from the DMA curves. It is observed that the T_g values corresponding to E'' maxima are fairly higher than those obtained from DSC analysis. The difference in T_g values is found to be about 25°C in the case of NR soft phase. A similar increase in T_g values of hard segment is also observed.

The relaxation temperature increases with hard segment content. A corresponding decrease in the height of the tanδ peak is also observed. These effects are prominent in the case of the two-shot samples.

Scanning electron microscopy (SEM)

Figure 13 is the scanning electron micrographs of tensile fracture surface of samples synthesized by the one-shot process and *Figure 14* is that of the two-shot products. All the micrographs display a two-phase behaviour giving rise to domain structures. No reliable information about the actual structure can be derived from the micrographs of low hard segment samples (*Figure 13a* and *Figure 14a*). Thus NR/1, 3-BDO (70/30) does not show the presence of domains. This may be due to the very small size of the domains, which are densely distributed in the NR matrix. When the hard segment is increased to 40% the phase separation becomes distinct but the domain morphology is not found to be well organized. In the micrographs of 50 wt% hard segment samples, the domain distribution is increased with a wen ordered structure. Micrographs of 70% hard segment samples show any number of cavities with an average size equal to 24.5 μm. It is noteworthy that the cavity size agrees with the average domain size observed in the other micrographs of almost comparable hard segment content. Hence it is likely that the cavities are formed by the pull out of the globules during tensile fracture. The soft segment phase appears as elongated along the edges of the cavities.

The polyurethane segments in all the samples are completely separated into hard phase, which is seen as almost spherical beads in the micrographs. Supercrystalline structures are practically absent in the micrograph, suggesting that the domains exhibit amorphous character. This is because of the inability of the hard segments to crystallize due to the

Table 5 Kinetic parameters for the decomposition of typical one-shot products

Sample	Activation energy, E (kJ mol^{-1})		Arrhenius parameter, A (s^{-1})		Entropy, ΔS (J mol^{-1} deg^{-2})	
	Stage 1	Stage 2	Stage 1	Stage 2	Stage 1	Stage 2
NR/1, 3-BDO (70/30)	77.79	111.36	1.367×10	3.980×10	−228.22	−221.06
NR/1, 3-BDO (60/40)	93.26	223.90	3.592×10	4.869×10^5	−220.63	−242.75
NR/1, 3-BDO (50/50)	101.51	284.99	6.746×10	8.065×10^7	−215.56	−200.25
NR/1, 3-BDO (40/60)	83.02	316.37	1.091×10	1.030×10^9	−230.60	−179.06
NR/1, 3-BDO (30/70)	86.96	267.40	2.532×10	5.974×10^6	−223.23	−255.93

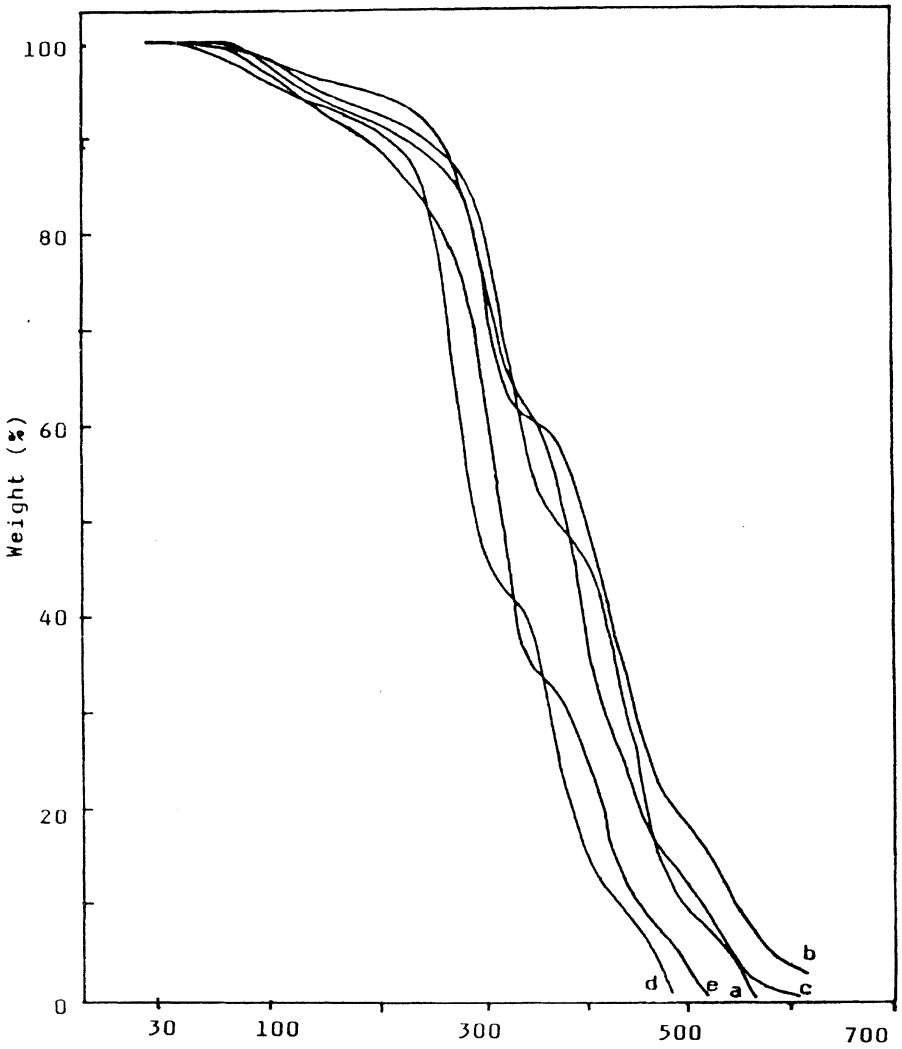

Figure 8 Thermograms of the two-shot products from TGA analysis: (a) NR/1, 3-BDO (60/40) (Shimadzu analyser); (b) NR/1, 3-BDO (50/50) (Shimadzu analyser); (c) NR/1, 3-BDO (40/60) (Shimadzu analyser); (d) NR/1, 3-BDO (70/30) (Shimadzu analyser).

Table 6 Kinetic parameters for the decomposition of typical two-shot products

Sample	Activation energy, E (kJ mol^{-1})		Arrhenius parameter, A (s^{-1})		Entropy, ΔS (J mol^{-1} deg^{-2})	
	Stage 1	Stage 2	Stage 1	Stage 2	Stage 1	Stage 2
NR/1, 3-BDO (70/30)	68.95	84.89	4.186	3.386	−238.24	−246.13
NR/1, 3-BDO (60/40)	86.51	80.37	2.926×10	1.894×10	−231.90	−240.55
NR/1, 3-BDO (50/50)	77.84	115.15	1.122×10	4.881×10	−229.89	−219.50
NR/1, 3-BDO (40/60)	82.61	126.64	1.733×10	1.876×10^2	−226.41	−207.81
NR/1, 3-BDO (30/70)	43.93	129.52	2.241×10	1.836×10^2	−261.92	−208.27

uneven disposition of the –NCO groups on the toluene diisocyanate molecule. This inhibits ordering and the subsequent chain alignment to form crystalline superstructures.

It is also noted from the micrograph that the hard domains form well-defined sharp boundaries within the matrix. This is an indication of its poor adhesion with the rubber matrix. The solubility parameters of the polyurethane and NR differ largely and hence segments of similar chemical composition segregate and form the respective domains.

The reaction mixture during the endcapping stage appeared clear and homogeneous. When the diol chain extender was added in solution it also mixed with the endcapped rubber solution retaining the homogeneity. It turned turbid only towards the end of the reaction. At this stage phase segregation begins, leading to domain formation. Since this process occurs in solution and the solvent is removed by slow evaporation during the casting process, better organization of hard segments occurs, leading to the formation of well-defined hard domains. Since the intermolecular force including hydrogen bonding is so strong in the hard phase, the domains appear as amorphous globules, as seen in the micrographs (*Figures 13 and 14*).

The relatively low mechanical properties of these block copolymers are caused by the high extent of phase separation existing in these materials. Due to poor bonding between the hard domains and the rubber matrix, debonding

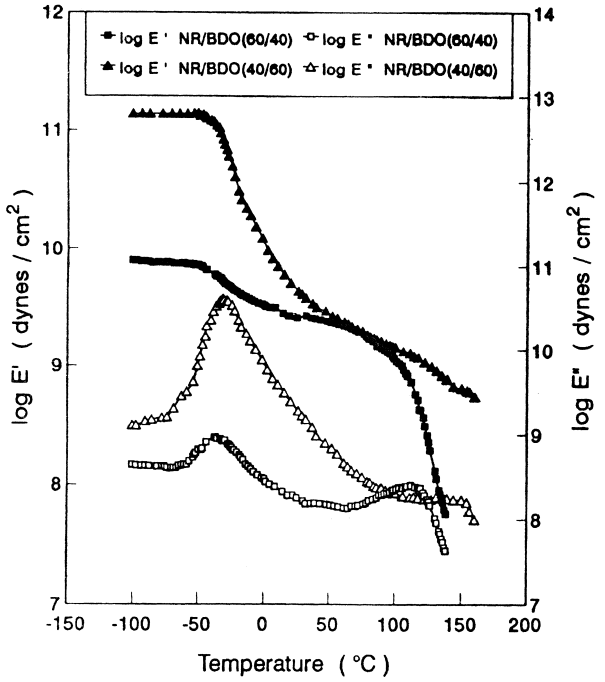

Figure 9 Temperature dependence of the storage modulus (E') and loss modulus (E'') of typical one-shot products.

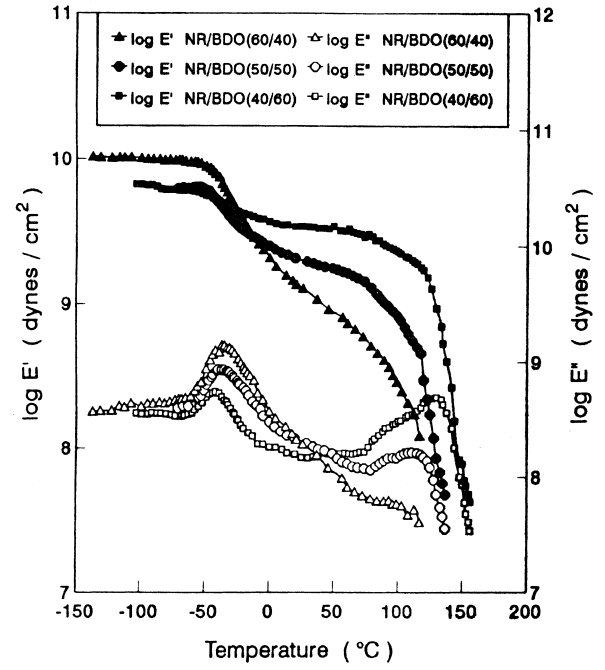

Figure 10 Temperature dependence of the storage modulus (E') and loss modulus (E'') of typical two-shot products.

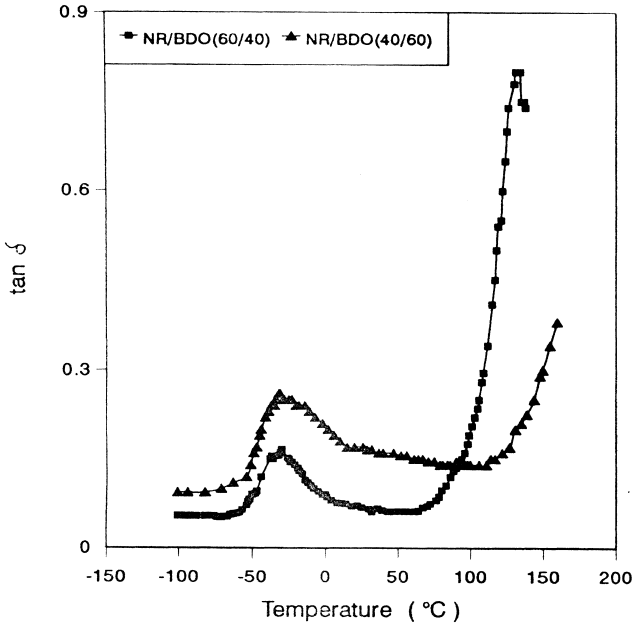

Figure 11 Temperature dependence of tanδ of typical one-shot products.

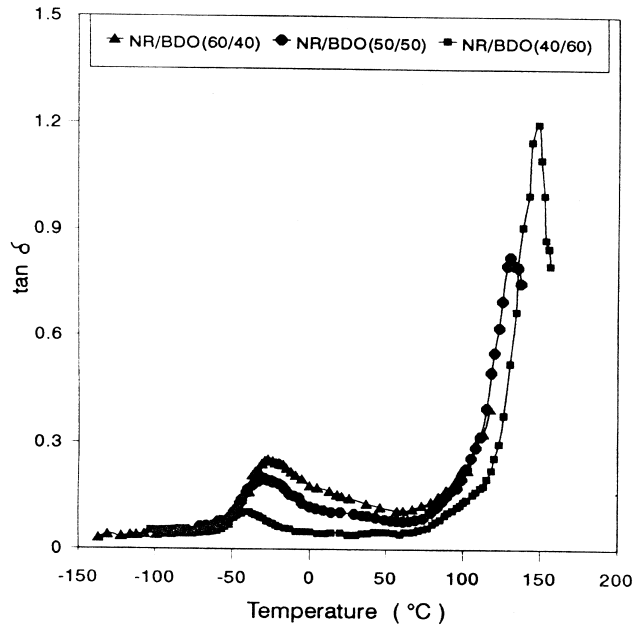

Figure 12 Temperature dependence of tanδ of typical two-shot products.

occurs at relatively low stress in both one-shot and two-shot samples during the tensile fracture, creating craters in the rubber matrix. This behaviour is contrary to that of conventional polyurethane elastomers which exhibit better tensile properties attributed to some extent of phase mixing.

The domain size, domain distribution and domain density with respect to hard segment content have been given in *Table 8*. The mean domain size increases from 4.98 to 25.30 μm as the hard segment content increases from 30 to 70% for the one-shot samples. A similar increase from 4.16 to 21.11 μm is observed in the case of two-shot samples. The size distribution within a given hard segment is found to be very wide. For example, in sample with 50% hard segment the variation of size is from 5.50 to 21.90 μm for two-shot samples and 6.60 to 27.20 μm for one-shot samples. The one-shot samples have a slightly higher particle size. This could be due to a less systematic way of chain extension that occurs during the one-shot process compared with the two-shot process. However, not much difference in sample morphology, domain size and distribution are observed between one-shot and two-shot samples. This indicates that the chain extension reaction taking place in solution proceeds more or less in a uniform manner irrespective of the method of synthesis.

Table 7 T_g values of the soft and hard segments from dynamic mechanical analysis

Sample	Soft segment T_g		Hard segment T_g	
	One-shot (°C)	Two-shot (°C)	One-shot (°C)	Two-shot (°C)
NR/1, 3-BDO (60/40)	−37.0	−36.5	110.8	112.2
NR/1, 3-BDO (50/50)	–	−35.5	–	118.2
NR/1, 3-BDO (40/60)	−32.4	−38.2	131.1	130.4

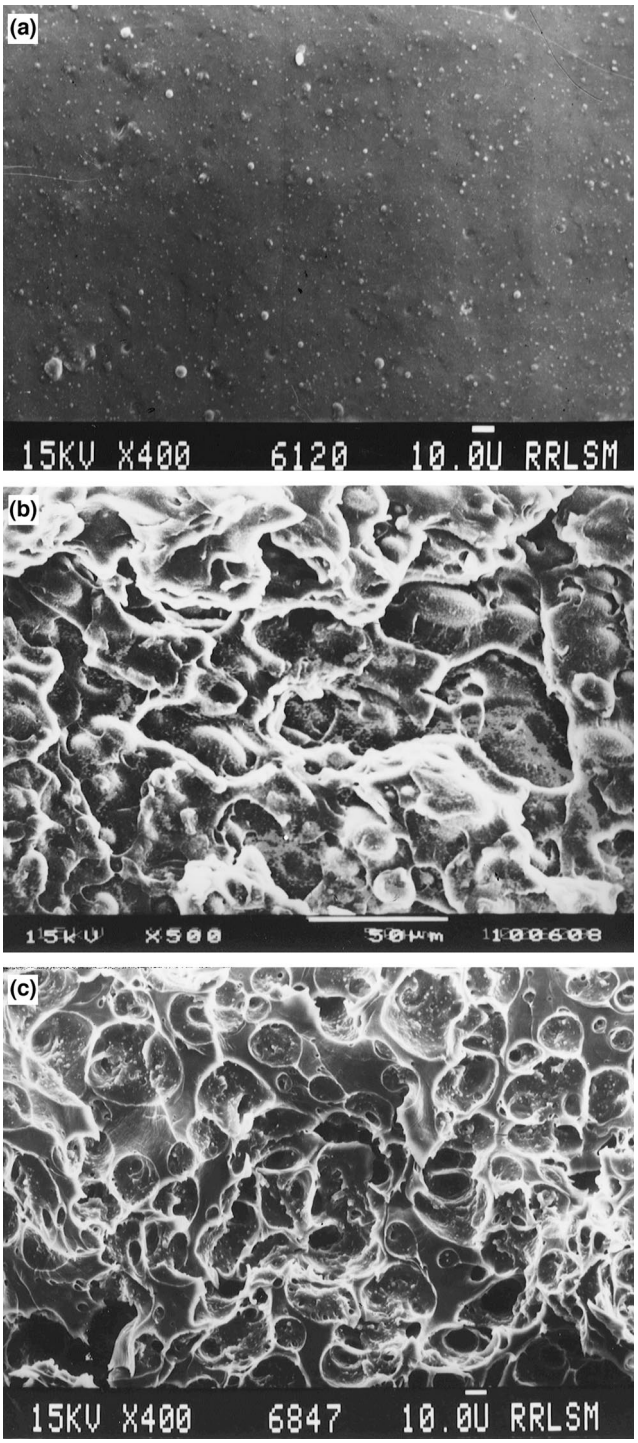

Figure 13 Scanning electron micrographs of typical one-shot products: (a) NR/1, 3-BDO (70/30); (b) NR/1, 3-BDO (50/50); (c) NR/1, 3-BDO; (30/70).

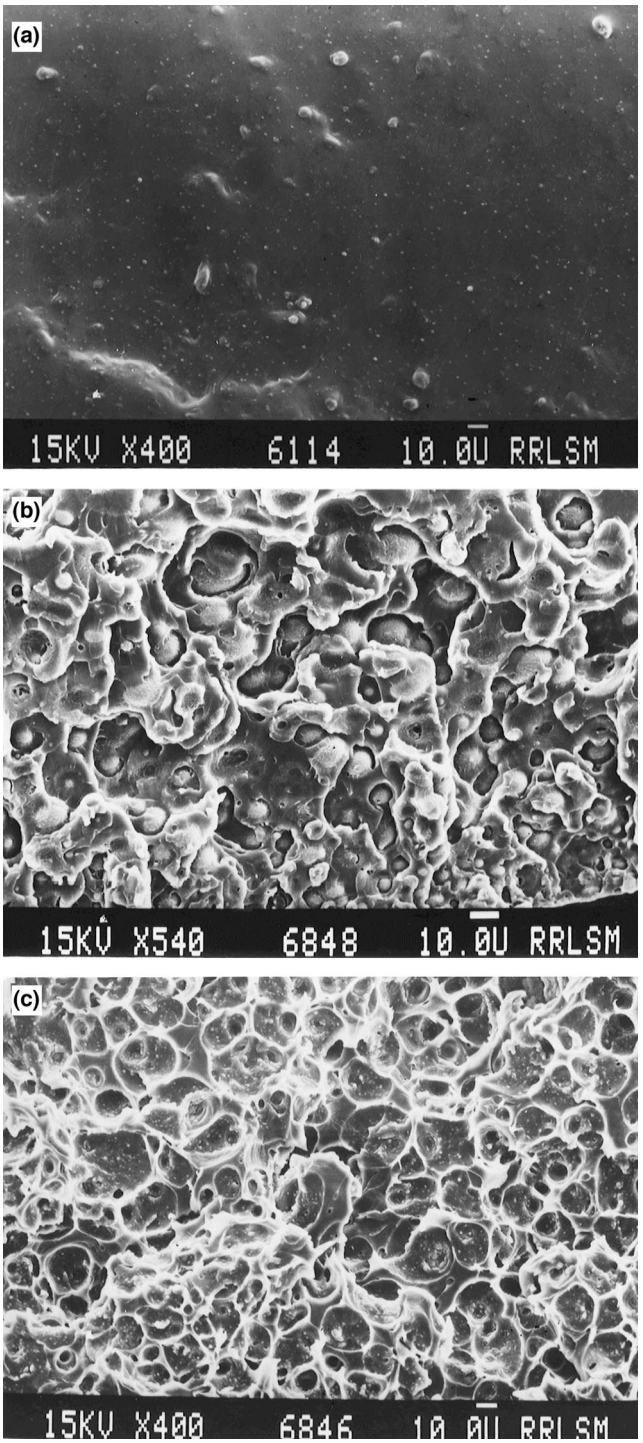

Figure 14 Scanning electron micrographs of typical two-shot products: (a) NR/1, 3-BDO (70/30); (b) NR1, 3-BDO (50/50); (c) NR/1, 3-BDO (30/70).

Table 8 Relationships between the hard segment content, the domain size and domain density.

Sample	Percentage of hard segment	Mean domain size (μm)		Domain density[a] (m^{-2})	
		One-shot	Two-shot	One-shot	Two-shot
NR/1, 3-BDO (70/30)	30	4.98	4.16	Not reliable	Not reliable
NR/1, 3-BDO (50/50)	50	18.60	15.52	9.80×10^8	16.43×10^8
NR/1, 3-BDO (30/70)	70	25.30	21.11	3.13×10^8	5.25×10^8

[a]Particle density is expressed as number per unit fracture surface area.

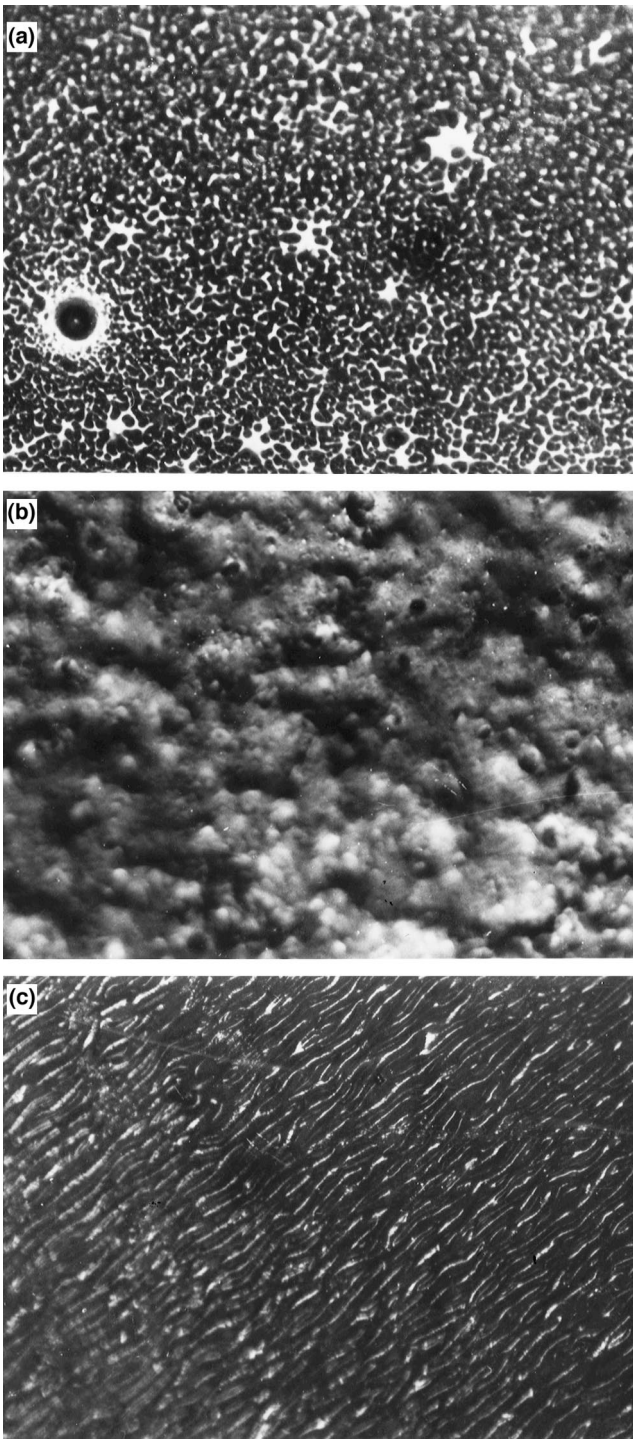

Figure 15 Optical micrograph of: (a) NR/1, 3-BDO (50/50) by one-shot process; (b) NR/1, 3-BDO (50/50) by two-shot process; (c) NR/1, 3-BDO (30/70) by two-shot process.

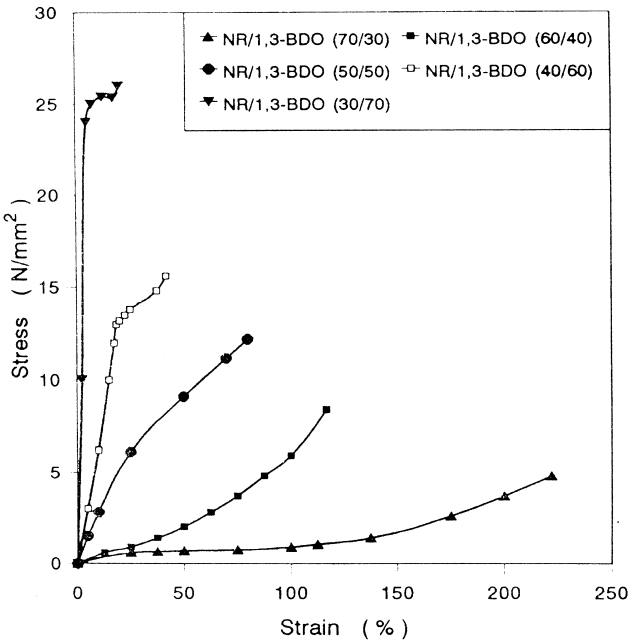

Figure 16 Stress–strain curves of the one-shot products.

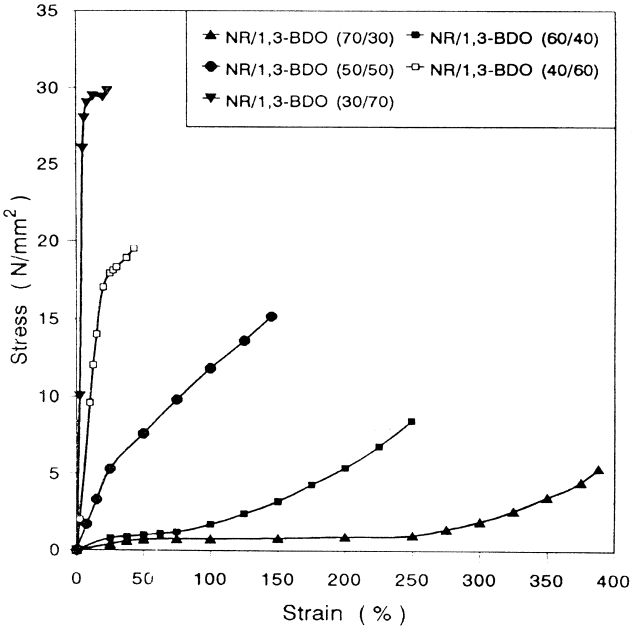

Figure 17 Stress–strain curves of the two-shot products.

Table 9 Tensile properties of the block copolymers

Sample	Tensile strength (N mm^{-2})		Elongation at break (%)	
	One-shot products	Two-shot products	One-shot products	Two-shot products
NR/1, 3-BDO (70/30)	4.80	5.38	222.37	388.0
NR/1, 3-BDO (60/40)	8.40	8.45	116.63	249.0
NR/1, 3-BDO (50/50)	12.20	15.18	80.33	145.0
NR/1, 3-BDO (40/60)	15.60	19.50	42.33	43.0
NR/1, 3-BDO (30/70)	25.93	29.80	18.00	23.0

Table 10 Tear strength of the two-shot products

Sample	Tear strength (N mm^{-2})
NR/1, 3-BDO (70/30)	17.01
NR/1, 3-BDO (60/40)	26.45
NR/1, 3-BDO (50/50)	35.59
NR/1, 3-BDO (40/60)	46.08
NR/1, 3-BDO (30/70)	70.67

Optical microscopy

The optical micrographs of NR1, 3-BDO (50/50) by one-shot and two-shot processes are shown in *Figure 15a* and *b*, respectively. Both the micrographs clearly exhibit micro-phase separation giving rise to domain structures. The black phase most likely represents the soft segments and the white phase is the hard segments. A network morphology is observed in both the samples. This is more pronounced in the micrograph of the two-shot samples with well-defined domains showing the uniformity in the distribution of hard segments in these samples. *Figure 15c* represents the micrograph of NR/1, 3-BDO (30/70) prepared by the two-shot method. An ordered lamellar structure is observed for this sample in which the soft segments are distributed in hard segment matrix. The ordered arrangement is again an indication of the uniformity of the block copolymer molecules prepared by the two-shot process.

Stress–strain behaviour

The stress–strain curves of the samples prepared by the one-shot and two-shot methods are given in *Figures 16 and 17*. In either case systematic changes are observed in the tensile properties with the hard segment content. In general, the initial modulus increases with an increase in the hard segment content. This is an indication of the greater rigidity of the samples imposed by the hard segments. These segments are less mobile and hence have much more difficulty in sliding past one another, showing greater rigidity. Ferguson *et al.*[25] explains the change in the initial modulus as something associated with phase change that occurs with the variation in the hard segment content. The elongation at break decreases with increasing hard segment. It is the continuous phase that dominates in the elongation behaviour.

Based on the tensile curves the samples have been divided into three categories. For examples, at lower hard segment concentration the materials behave like quasi-elastomers. As the hard segment content increases the system changes from quasi-elastomer to tough plastics.

The tensile strength of the samples increases to a greater extent when the hard segment content is increased. However, the block copolymers under present study possess only lower tensile properties compared with those of conventional polyurethanes. The reason is attributed to the absence of phase mixing between hard and soft segment and the compositional heterogeneity of the hard segments.

The various values obtained in the tensile studies are tabulated in *Table 9*. A direct comparison of the values for the two types of samples shows that the two-shot samples exhibit better ultimate properties. The reason for the inferior mechanical properties of the one-shot material is attributed to the less systematic ordering of the different segments in the samples.

Tear strength

The tear strength of the samples prepared by the two-shot process has been tabulated in *Table 10*. The values tend to increase with increase in the hard segment content. However, these materials exhibit low tear strength in comparison with other phase separated elastomeric materials.

CONCLUSION

The segmented block copolymers synthesized by both one-shot and two-shot processes are amorphous materials. DSC and rheovibron measurements indicate that the glass transition temperature of the soft segment is invariant with increasing polyurethane content, which shows that phase segregation is very nearly complete. Since TDI and 1, 3-BDO form amorphous hard segments, the driving force for phase separation is the extreme incompatibility of the nonpolar soft segment and the strongly polar hard segment units. Absence of any hydrogen bonding between the soft and hard segments further increases the incompatibility between the phases. The two-stage thermal decomposition of the materials is further evidence for the two-phase morphology.

The systematic variation of the hard segment T_g with the variation in hard segment content, as evidenced by DSC and DMA, is also reflected in stress–strain properties whereby the material changes from a quasi-elastomer to a brittle plastic. This is unquestionably due to an inversion of the continuous and dispersed phases in the system which occurs at approximately 50–60 wt% of hard segment. The SEM and optical microscopic studies further confirm this morphological variation.

Another significant feature of this study is that the two-shot materials exhibit more systematic ordering of segments and hence better mechanical properties.

REFERENCES

1. Bengston, B., Feger, C., MacKnight, W. J. and Schneider, N. S., *Polymer*, 1985, **26**, 895.
2. Koberstein, J. T. and Stein, R. S., *J. Polym. Sci.*, 1983, **21**, 1439.
3. Chen-Tsai, C. H. Y., Briber, R. M., Thomas, E. L., Xu, M. and MacKnight, W., *J. Polymer*, 1983, **24**, 1334.
4. Xu, M., MacKnight, W. J., Chen, C. H. Y. and Thomas, E. L., *Polymer*, 1983, **24**, 1327.

5. Estes, G. M., Cooper, S. L. and Tobolsky, A. V. J., *Macromol. Sci.*, 1970, **C4**, 313.
6. Francis, D. J., Ravindran, T. and Nayar, M. R. G. in *32nd Annual Polyurethane Technical Marketing Conference*, 1989, p. 373.
7. Chen-Tsai, C. H. Y., Thomas, E. L., MacKnight, W. J. and Schneider, N. S., *Polymer*, 1986, **27**, 659.
8. Serrano, M., MacKnight, W. J., Thomas, E. L. and Ottino, J. M., *Polymer*, 1987, **28**, 1667.
9. Serrano, M., MacKnight, W. J., Thomas, E. L. and Ottino, J. M., *Polymer*, 1987, **28**, 1674.
10. Xu, M., MacKnight, W. J., Chen-Tsai, C. H. Y. and Thomas, E. L., *Polymer*, 1987, **28**, 2183.
11. Schneider, N. S. and Matton, R. W., *Polym. Engng Sci.*, 1979, **19**(15), 1122.
12. Brunette, C. M., Hsu, S. L., Rossman, M., MacKnight, W. J. and Schneider, N. S., *Polym. Engng Sci.*, 1981, **21**(11), 668.
13. Fu, B., MacKnight, W. J. and Schneider, N. S., *Rubber Chem. Technol.*, 1986, **59**, 896.
14. Camberlin, Y. and Pascault, J. P., *J. Polym. Sci. Polym. Chem. Edn*, 1983, **21**, 415.
15. Camberlin, Y. and Pascault, J. P., *J. Polym. Sci. Polym. Phys. Edn*, 1984, **22**, 1835.
16. Speckhard, T. A., Gibson, P. E., Cooper, S. L., Chang, V. S. C. and Kennedy, J. P., *Polymer*, 1985, **26**, 55.
17. Speckhard, T. A., Hwang, K. K. S., Cooper, S. L., Chang, V. S. C. and Kennedy, J. P., *Polymer*, 1985, **26**, 70.
18. Ravindran, T., Nayar, M. R. G. and Francis, D. J., *Makromol. Chem. Rapid Commun.*, 1986, **7**, 159.
19. Ravindran, T., Nayar, M. R. G. and Francis, D. J., *J. Appl. Polym. Sci.*, 1991, **42**, 325.
20. Paul, C. J. and Nair, M. R. G., *Ind. J. Nat. Rubber Res.*, 1992, **5**(1–2), 199.
21. Ravindran, T., Nayir, M. R. G. and Francis, D. J., *J. Appl. Polym. Sci.*, 1988, **35**, 1227.
22. Sung, P. C. S., Hu, C. B. and Wu, C. S., *Macromolecules*, 1980, **13**, 111.
23. Madhusudanan, P. M., Yusuf, K. K. M. and Nair, C. G. R., *J. Thermal Anal.*, 1975, **8**, 311.
24. Satava, V., *Thermochim. Acta*, 1971, **2**, 423.
25. Ferguson, J. and Ahmad, N., *Eur. Polym. J.*, 1977, **13**, 865.